Fusing a Planar Group to a π-Bowl: Electronic and Molecular Structure, Aromaticity and Solid-State Packing of Naphthocorannulene and its Anions

Title: Fusing Planar Group to a pi-Bowl: Electronic and Molecular Structure, Aromaticity and Solid State Packing of Naphthocorannulene and its Anions

Authors: Zheng Zhou; Sarah Spisak; Qi Xu; Andrey Rogachev; Zheng Wei; Massimo Marcaccio; Marina A. Petrukhina

To be cited as: 10.1002/chem.201705814

Link to VoR: https://doi.org/10.1002/chem.201705814

Fusing Planar Group to a π-Bowl: Electronic and Molecular Structure, Aromaticity and Solid State Packing of Naphthocorannulene and its Anions

Zheng Zhou,[a] Sarah N. Spisak,[a] Qi Xu,[b] Andrey Yu. Rogachev,[b,*] Zheng Wei,[a] Massimo Marcaccio[c] and Marina A. Petrukhina[a,*]

[a] *Department of Chemistry, University at Albany, State University of New York, Albany, NY 12222, USA.* *mpetrukhina@albany.edu

[b] *Department of Chemistry, Illinois Institute of Technology, Chicago, IL 60616, USA.* *arogache@iit.edu

[c] *Department of Chemistry "G. Ciamician", University of Bologna, Via Selmi 2, 40126, Bologna, Italy*

Abstract

Molecular and electronic structure, reduction electron transfer and coordination abilities of a polycyclic aromatic hydrocarbon (PAH) having a planar naphtho-group fused to the corannulene bowl have been investigated for the first time using a combination of theoretical and experimental tools. A direct comparison of naphtho[2,3-*a*]corannulene ($C_{28}H_{14}$, **1**) with parent corannulene ($C_{20}H_{10}$, **2**) revealed the effect of framework topology change on electronic properties and aromaticity of **1**. The presence of two reduction steps for **1** was predicted theoretically and confirmed experimentally. Two reversible one-electron reduction processes with the formal reduction potentials at –2.30 V and –2.77 V *vs*. $Fc^{+/0}$ were detected by cyclic voltammetry (CV) measurements, demonstrating accessibility of the corresponding mono- and dianionic states of **1**. The products of the mono- and doubly-reduced napththocorannulene were prepared using chemical reduction with Group 1 metals and isolated

as sodium and rubidium salts. Their X-ray diffraction study revealed the formation of "naked" mono- and dianions crystallized as solvent-separated ion products with one or two sodium cations as $[Na^{+}(18\text{-crown-6})(THF)_2][C_{28}H_{14}^{-}]$ and $[Na^{+}(18\text{-crown-6})(THF)_2]_2[C_{28}H_{14}^{2-}]$ (**3**·THF and **4**·THF, respectively). The dianion of **1** was also isolated as a contact-ion complex with two rubidium countercations, $[\{Rb^{+}(18\text{-crown-6})\}_2(C_{28}H_{14}^{2-})]$ (**5**·THF). The structural consequences of adding one and two electrons to the carbon framework of **1** are compared for **3**, **4** and **5**. Changes in aromaticity and charge distribution stemming from the stepwise electron acquisition are discussed based on DFT computational study.

Keywords: non-planar polyarenes · π-bowls · aromaticity · molecular structure · chemical reduction · X-ray diffraction · carbanions

TOC:

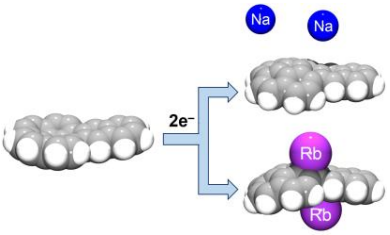

Introduction

Metalation of curved carbon surfaces attracts special attention of organometallic and materials chemists due to fundamental interest and potential applications.[1] Starting from extensive exploration of fullerenes,[2] these studies have recently shifted to the non-planar fragments of fullerenes (also referred to as open geodesic polyarenes,[3] buckybowls,[4] molecular[5] or π-bowls [6]). The latter represent a very interesting class of π-conjugated ligands since their convex (*exo*) and concave (*endo*) faces are readily accessible for metal binding. Due to this unique versatility π-bowls have shown a great variation of coordination modes.[7] In addition, their binding abilities can be further enhanced through stepwise electron acquisition.[8] We have recently developed the preparation procedures that allowed the isolation of crystalline products of the bowl-shaped corannulene, $C_{20}H_{10}$ (Scheme 1a), upon step-wise electron addition. Notably, the resulting set of consequently reduced corannulene carbanions, $C_{20}H_{10}^{n-}$ (n = 1–4), exhibits distinctly different metal binding preferences. Based on X-ray crystallographic studies, we have demonstrated that mono- and doubly-reduced corannulene can form solvent-separated or contact-ion pairs with alkali metal ions in the solid state,[9] while the electron-rich triply- and tetrareduced corannulene anions self-assemble into unique sandwich-type aggregates with a record number of metal ions encapsulated.[10] The first study of sumanene reactions with Group 1 metals also revealed the tendency of sumanenyl trianions to self-assemble into a novel supramolecular sandwich with multiple K^+ ions.[11] These works demonstrated that the charge, size and symmetry of a π-bowl can affect the type of supramolecular assembly, prompting us to investigate the bowl-shaped polycyclic aromatic hydrocarbons (PAHs) having large surface area and different carbon framework topologies.[12] In this regard, fusion of a planar naphtho-group to the corannulene core provides a unique PAH ($C_{28}H_{14}$ **1**, Scheme 1b) with dual potential sites for reduction and metal coordination. Both fragments are known to exhibit rich individual redox chemistry with naphthalene forming an electron-rich dianion[13] and corannulene undergoing four one-electron reduction steps.[8] Although the synthesis of $C_{28}H_{14}$ was reported back in 2001,[14] no studies of its molecular structure and solid state packing have been accomplished since then. In 2006, *in situ* chemical reduction of **1** was probed by solution NMR spectroscopy,[15] but no products were isolated in the solid state, leaving questions regarding the overall structures, potential metal binding sites and geometry transformations of the resulting carbanions open.

Very recently, remarkable examples of large carbon-rich PAHs having planar and bowl-shaped fragments fused together have been reported,[16] indicating the important role of the size and curvature of such π-systems in modulating their properties. Despite these successful efforts directed toward blending planar and curved parts, investigations of the metal-induced reduction processes and outcomes of multi-electron addition to such unique hybrid π-systems have yet to be initiated.

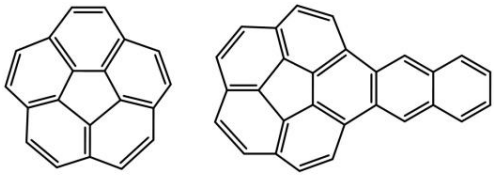

Scheme 1. Corannulene, $C_{20}H_{10}$ (*a*), and naphtho[2,3-*a*]corannulene, $C_{28}H_{14}$ (*b*).

Herein we provide the first comprehensive investigation of structure and properties of naphtho[2,3-*a*]corannulene ($C_{28}H_{14}$, **1**) using a combination of X-ray crystallography, CV measurements and DFT calculations. The chemical reduction of **1** with Group 1 metals was also investigated; the resulting mono- and doubly-reduced carbanions were isolated as the corresponding alkali metal salts and fully characterized.

Results and Discussion

DFT: Neutral Naphthocorannulene

Since no evaluation of molecular and electronic features of napththo[2,3-*a*]corannulene ($C_{28}H_{14}$, **1**) has been accomplished, we started with an analysis of its structure and properties and compared those with parent corannulene ($C_{20}H_{10}$, **2**), using a set of modern computational tools (see ESI for more details). We observed that fusion of the naphthalene fragment to the corannulene core results in notable changes of the bowl-shaped part of the molecule. First, it reduces the bowl depth to 0.827 Å *vs*. that of 0.875 Å for corannulene.[17] Second, the bowl flattening is expected to be associated with a lower energy barrier of the bowl-to-bowl inversion. Indeed, it is found to be +7.80 kcal/mol for neutral $C_{28}H_{14}$, which is lower than that in $C_{20}H_{10}$

(+9.98 kcal/mol). Next, the charge distribution in $C_{28}H_{14}$ is less symmetric (Figure 1) than that in corannulene.[12a] Specifically, two separate negatively-charged areas (one is localized on the bowl part and the other one is mostly concentrated on the naphtho-group) can be clearly seen. In general, such distribution may be indicative of possible charge separation during excitation and/or reduction/oxidation.

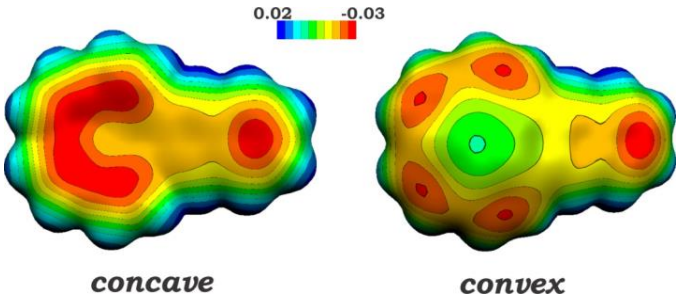

Figure 1. MEP maps of neutral $C_{28}H_{14}$ molecule.

Further support for the above statement comes from analysis of the molecular orbital (MO) diagram of $C_{28}H_{14}$ (Figure 2). The highest occupied MO (HOMO) is mostly localized on the planar naphtho-group, whereas HOMO-1 and HOMO-2 are concentrated on the bowl part. Important feature of the electronic structure of $C_{28}H_{14}$ also includes different localization of HOMO and LUMO orbitals (Figure 2). In contrast to the above HOMO, the LUMO is mainly localized on the corannulene part.

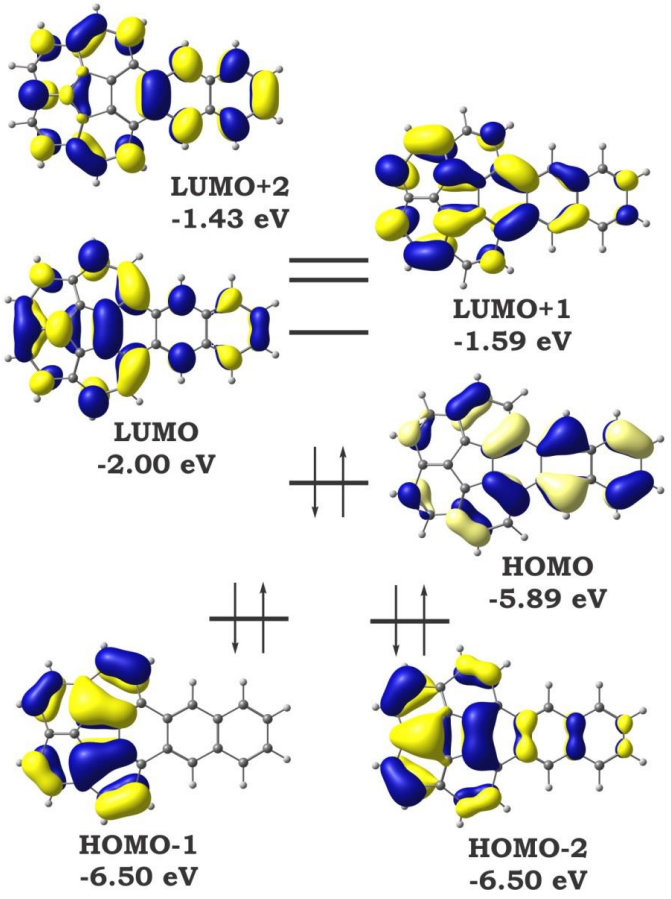

Figure 2. MO diagram of neutral $C_{28}H_{14}$ (PBE0/cc-pVTZ).

From the energy point of view, HOMO-1 and HOMO-2 are degenerated. Similarly, LUMO+1 and LUMO+2 are separated by only 0.16 eV. The Δ(HOMO-LUMO) gap of **1** is 3.89 eV, making $C_{28}H_{14}$ a significantly better acceptor than corannulene (Δ(HOMO-LUMO) = 4.71 eV) and comparable to the recently studied indacenopicene, $C_{26}H_{12}$ (3.65 eV).[12a] At the same time, the LUMO of $C_{28}H_{14}$ (-2.00 eV) lies notably higher than that of $C_{26}H_{12}$ (-2.42 eV) but lower than that of $C_{20}H_{10}$ (-1.77 eV). In contrast, HOMO (-5.89 eV) of **1** is significantly higher than that in both, corannulene (-6.48 eV) and indacenopicene (-6.07 eV). Thus, $C_{28}H_{14}$ is expected to be a better donor with respect to Lewis acidic agents.

Addition of naphtho-group to the corannulene bowl has also resulted in the significant perturbation of the aromatic π-system. The induced changes were carefully monitored through a set of aromaticity descriptors of different nature (Table 1, see ESI for details), all consistently

revealing the same trends. Briefly, while the anti-aromatic character of the central 5-membered ring A remains essentially the same as in $C_{20}H_{10}$, the behavior of 6-membered rings in $C_{28}H_{14}$ is now different. The aromaticity of rings C and D has almost unchanged in comparison with $C_{20}H_{10}$, while the ring B is better described as non-aromatic (Table 1). In contrast, the neighboring rings E and F of the naphtho-fragment show a strong aromatic character.

In order to further investigate delocalization and magnetic currents in **1**, the ACID maps were constructed for the total electron density as well as for its π-component (Figure 3). Strong paratropic ring current is found for the 5-membered ring, in full agreement with its anti-aromatic behavior (as evidenced by a magnetic aromaticity descriptor such as NICS). At the same time, π-delocalization at the periphery covers the whole molecule of **1**, including all *rim*-bonds of corannulene and naphthalene parts. This delocalization is diatropic in nature and, importantly, it only slightly touches the ring B, thus explaining its non-aromaticity (Table 1). The non-aromatic character of the ring B can be also understood in the term of Clar's rule.[18]

Table 1. Aromatic indexes calculated for neutral $C_{28}H_{14}$ and $C_{20}H_{10}$ (PBE0/cc-pVTZ).

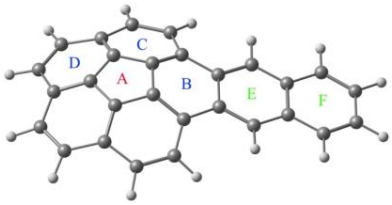

System	Ring	HOMA	NICS	AIM Analysis		Fuzzy Space	
				PDI	FLU	PDI	FLU
C_6H_6		1.000	-8.21	0.105	0.000	0.106	0.000
C_5H_6		-0.622	-3.43		0.054		0.057
$C_{28}H_{14}$	A	0.862	8.76		0.029		0.040
	B	0.095	0.10	0.029	0.027	0.031	0.035
	C	0.802	-6.30	0.065	0.011	0.066	0.016
	D	0.742	-5.91	0.057	0.015	0.059	0.020
	E	0.678	-8.88	0.065	0.010	0.066	0.015
	F	0.821	-8.10	0.072	0.011	0.074	0.013
$C_{20}H_{10}$	B	0.702	-6.43	0.059	0.014	0.060	0.019

	A	0.818	9.22	-	0.026	-	0.038

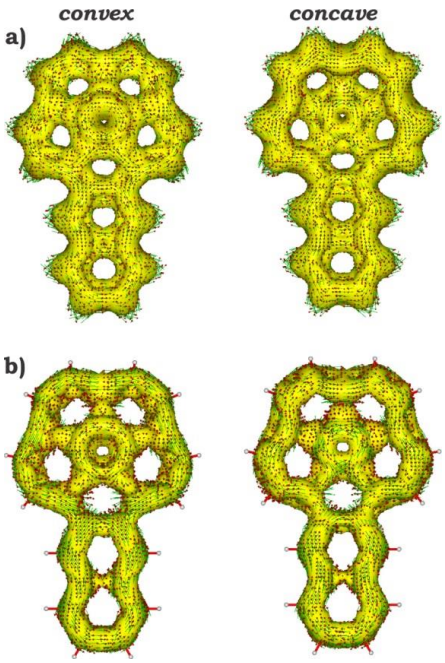

Figure 3. ACID isosurfaces (*a*) and their π-contributions (*b*) for neutral $C_{28}H_{14}$ molecule. Current density vectors are plotted onto the ACID surfaces to indicate dia- and paratropic ring currents.

DFT and CV: Mono- and Dianionic States of $C_{28}H_{14}$

Based on its MO diagram, **1** should readily accept up to two electrons in step-wise reduction processes. Addition of one and two electrons to the $C_{28}H_{14}$ molecule results in a notable re-shaping of the electron density distribution. As evidenced by the MEP maps (Figure 4), the negative charge in both mono- and double-reduced carbanions is exclusively localized over the bowl-shaped part. This finding is in full agreement with the calculated MO diagram of neutral $C_{28}H_{14}$ (Figure 2), as it perfectly correlates with the topology of HOMO.

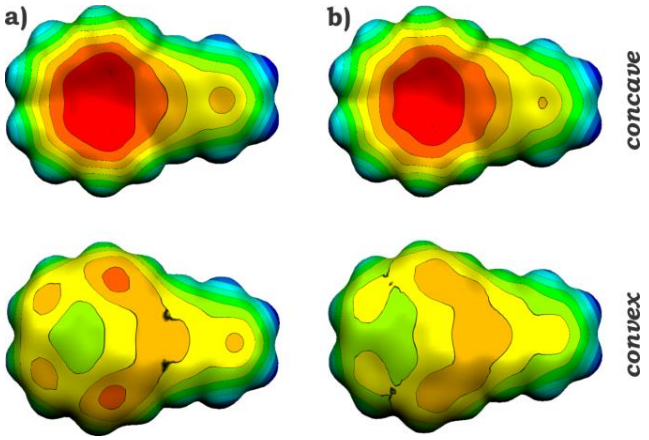

Figure 4. MEP maps of the mono- (*a*) and di-anion (*b*) of $C_{28}H_{14}$.

The above theoretical predictions concerning the electron-accepting properties of **1** are fully supported by the electrochemical investigation of the reduction processes at 25 °C in THF. The cyclic voltammetric (CV) curves, reported in Figure 5, show two reductions in the available potential window of the electrolyte solution (which extends up to about -3.5 V). The two subsequent electron transfers occur with $E_{½}$ values of –2.30 V and –2.77 V (*vs*. $Fc^{+/0}$), respectively, and both are completely reversible one-electron processes. The stability of the electrochemically generated mono- and dianions of **1** was evaluated by checking the voltammetric reversibility at different sweep rates (in the range 0.4 V/s to 100 V/s). This further evidenced that even in the longest timescale explored (few seconds) the two reduction products are stable. In addition, no other kind of chemical reactivity was highlighted at shorter (millisecond range) timescale.

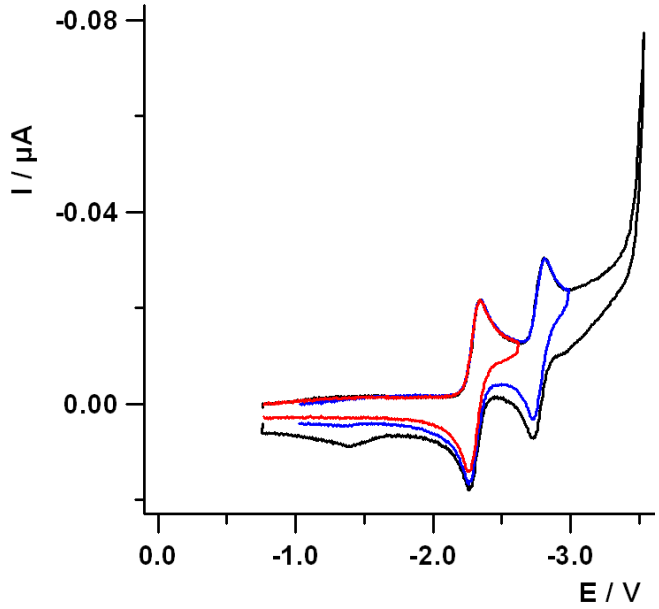

Figure 5. Cyclic voltammetric curves of 0.7 mM of **1** in 0.08 M TBAH/THF solution. Working electrode: Pt (125 µm, diameter); *T* = 25 °C; Sweep rate: 1 V/s.

The first reduction potential of **1**, compared to that of the parent corannulene, is 0.17 V less negative. The electrochemical energy gap between the two processes measures 0.47 eV, which is 0.11 eV lower than the corresponding separation for corannulene (0.58 eV).[19] This can be rationalized on the basis of a larger π-conjugation through the naphthalene moiety (*vide supra*). Notably, the energy difference between the first and second reduction potentials has a value quite close to the theoretical LUMO-LUMO+1 separation (Figure 2) for the neutral compound.

$C_{28}H_{14}$: X-ray Crystallographic Study

Since the solid state structure of $C_{28}H_{14}$ remained unknown, we started with crystallization of naphtho[2,3-*a*]corannulene. We selected an efficient microscale gas-phase sublimation/deposition method[20] for crystal growth, as it allows one to avoid encapsulation of any solvent molecules into the crystal lattice.[21] Deposition of **1** at 160 °C in a small evacuated and sealed glass ampule over 2 days afforded pale yellow needles in high yield. An X-ray structural characterization revealed the molecular structure (Figure 6) and crystal packing of **1**

(Figure 7). The core parameters of **1** (Table 2) are compared with those of corannulene and naphthalene (See ESI, Table S2). The depth of corannulene bowl in **1** of 0.813(7) Å is reduced *vs* that of parent corannulene (0.875(2) Å), in accord with the above theoretical predictions. The calculated POAV angles for **1** (Table S3) also illustrate the reduction of curvature of the bowl-part compared to corannulene.

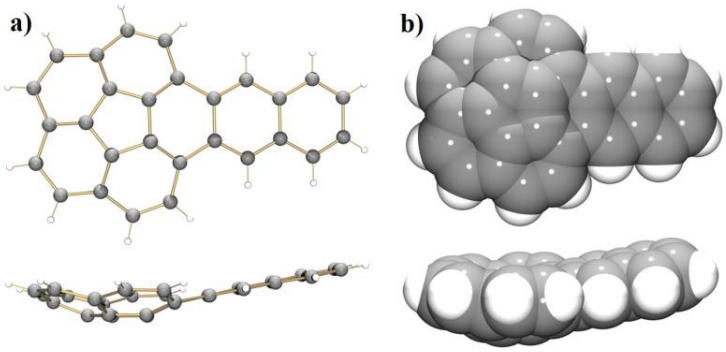

Figure 6. Molecular structure of **1**, top and side views in ball-and-stick (*a*) and space-filling models (*b*).

In the solid state structure of **1**, the one-dimensional columns are unidirectional with a bowl slip of 1.985 Å (Figure S21). The two different stacking distances can be measured, averaging at 3.333 Å (Figure 7a). The 1D stacks are linked together into an extended 2D network (Figure 7b) through intermolecular C–H$\cdots\pi$ interactions ranging from 2.617 to 2.775 Å (Figure S22).

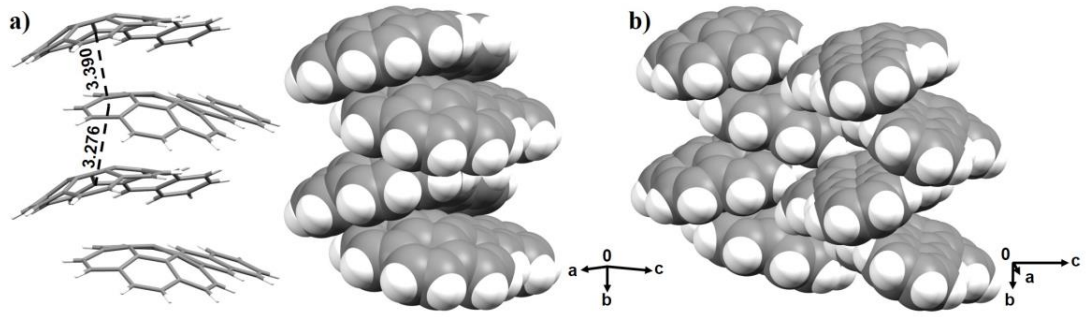

Figure 7. Solid state packing of **1**, 1D column in capped-stick and space-filling models (*a*) and 2D packing (*b*).

Notably, the solid-state packing of **1** is different from that of $C_{20}H_{10}$, as the latter is dominated by C–H···π interactions with no long-range 1D stacking of corannulene bowls.[17] However, a slipped columnar packing similar to that observed in **1** has been previously seen in the crystal structures of dibenzo[*a*,*g*]corannulene and other corannulene-based bowls.[22]

Chemical Reduction and X-ray Crystallographic Study of Carbanions

For the next step, we moved to investigation of the chemical reduction behavior of **1**. Consistently with the computational and electrochemical studies, we observe that reduction of $C_{28}H_{14}$ with Group 1 metals proceeds through two distinctive steps. The addition of an excess of alkali metal to **1**, in THF, allows the generation of a deep brown color associated with $C_{28}H_{14}^{-}$, which subsequently undergoes further reduction to form a dull brown-green solution of $C_{28}H_{14}^{2-}$ (Figures S1-S4). Based on these observations, we targeted the isolation of crystalline products of both mono- and doubly-reduced states of **1**. We primarily chose sodium metal for the first chemical reduction study because it is well known to result in the formation of "naked" carbanions.[9b,23] This should allow us to analyze the geometric perturbations of carbon framework of **1** upon acquisition of one and two electrons without the influence of direct metal binding.

The first product, $[Na^{+}(18\text{-crown-6})(THF)_2][C_{28}H_{14}^{-}]$ (**3**), was prepared by the controlled reduction of $C_{28}H_{14}$ with Na metal in the presence of 18-crown-6 ether in THF. The product was crystallized by slow diffusion of hexanes into a THF solution at 5 °C. Dark brown blocks of (**3**·THF) were isolated in moderate yield after 4 days. In **3** (Figure 8a), the sodium ion is coordinated by one axial 18-crown-6 ether ($Na\cdots O_{crown}$, 2.681(5)–2.874(6) Å) and two capping THF molecules ($Na\cdots O_{THF}$, 2.282(6) and 2.357(6) Å), with all Na···O distances being close to those previously reported.[7b,9b] The observed full encapsulation of sodium cation precludes its binding to the monoanion of **1**. Notably, the bowl depth of the "naked" $C_{28}H_{14}^{-}$ core in **3** (0.816(10) Å) remains essentially unchanged when compared to the neutral ligand (0.813(7) Å).

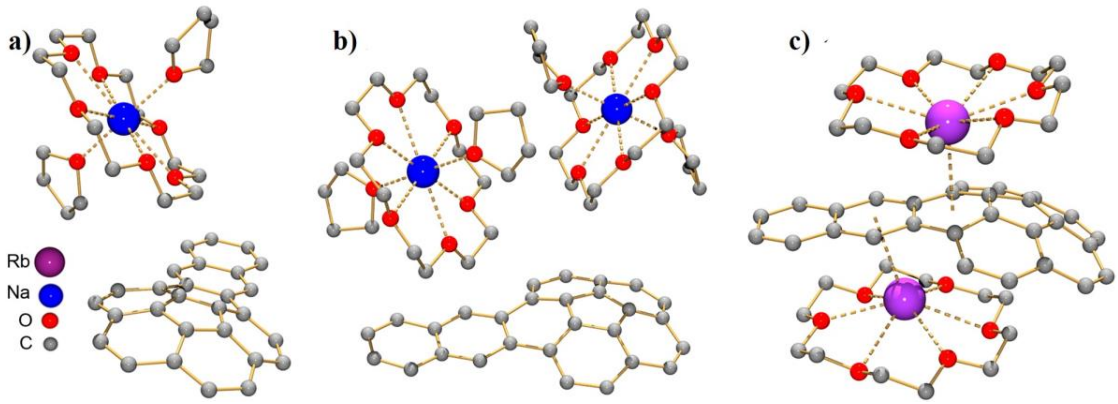

Figure 8. Molecular structures of **3** (*a*), **4** (*b*), and **5** (*c*). All hydrogen atoms are removed for clarity.

We have isolated and structurally characterized the dianion of **1** crystallized with two sodium countercations, $[Na^{+}(18\text{-crown-6})(THF)_2]_2[C_{28}H_{14}^{2-}]$ (Figure 8b, **4**). In **4**, both sodium ions are solvent-separated from the $C_{28}H_{14}^{2-}$ core, thus allowing us to analyze the effect of the acquisition of two electrons by **1** without interfering metal binding effects. The two-fold reduction results in a shallower depth of the corannulene bowl when compared to the parent molecule (0.794(2) Å *vs*. 0.813(7) Å).

Similarly to **3**, the Na^{+} ions are axially bound by one 18-crown-6 ether molecule ($Na\cdots O_{crown}$, 2.639(2)–2.935(3) Å) and capped by two THF molecules ($Na\cdots O_{THF}$, 2.317(5) and 2.337(2) Å) with all Na···O distances being close to those previously reported. In the solid state structure of **4** (Figure 9a), several C–H···π contacts between the $C_{28}H_{14}^{2-}$ dianion with the neighboring 18-crown-6 ether molecules ranging over 2.601(2)–2.897(2) Å can be identified.

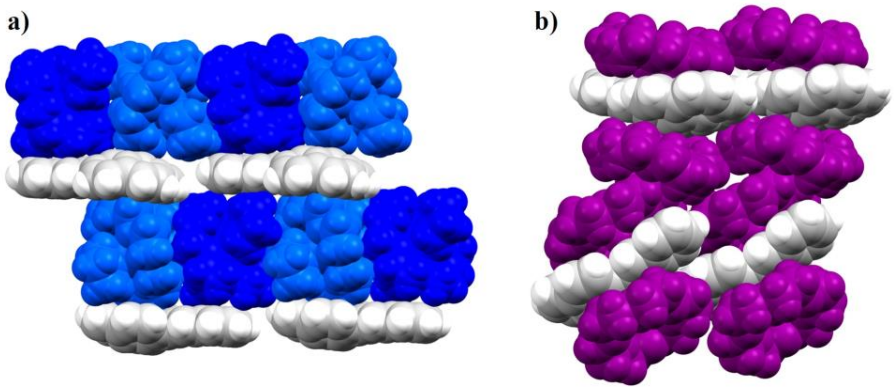

Figure 9. Solid state packing in **4** (*a*) and **5** (*b*), space filling models. The [Na^+(18-crown-6)$(THF)_2$] moieties are shown in different shades of blue, while [Rb^+(18-crown-6)] ions are purple.

In addition, we have prepared the dianion of **1** by the reduction of $C_{28}H_{14}$ with rubidium metal in the presence of 18-crown-6 ether. The resulting single crystals were obtained upon slow diffusion of hexanes into a THF solution at 5 °C. An X-ray diffraction study revealed the formation of the contact-ion complex, [{Rb^+(18-crown-6)}$_2$($C_{28}H_{14}^{2-}$)] (**5**·THF). In contrast to **4**, where no metal binding was observed, both rubidium ions are coordinated to the $C_{28}H_{14}^{2-}$ core (Figure 8c). One Rb^+ ion binds the six-membered ring B of the corannulene bowl in a convex (*exo*) fashion (Rb···C_{exo}, 3.187(6)–3.411(7) Å), while the second one interacts with the E ring approaching the planar naphtho-group from the opposite direction (Rb···C_{endo}, 3.191(6)–3.659(6) Å). The distances from these rubidium ions to the benzene ring centroids are 3.107(7) Å and 2.997(6) Å, respectively. For comparison, the distance of the Rb^+ ion to the six-membered ring centroid of $C_{20}H_{10}^-$ is 3.040(3) Å.[9a] Each Rb^+ ion is also coordinated by one 18-crown-6 ether molecule (Rb···O, 2.783(14)–3.100(5) Å). Overall, the Rb···O distances are close to those previously reported for the salts of different carbanions crystallized with Rb^+ ions capped by crown ethers.[9a,b,d,24]

In the solid state structure of **5** (Figure 9b), there are additional intermolecular contacts that include side π–π interactions between two neighboring $C_{28}H_{14}^{2-}$ anions (*ca*. 2.33 Å). The shortest intermolecular C–H···π interaction between $C_{28}H_{14}^{2-}$ and the adjacent 18-crown-6 ether molecule is found at 2.84 Å.

Based on the structures of dianions in **4** and **5**, the acquisition of two electrons by **1** results in elongation of the rim and spoke C–C bonds when compared to neutral $C_{28}H_{14}$ (Tables 2, S3). The C–C bond at the junction of naphthalene and corannulene parts is notably shortened upon the two electrons addition (**1**: 1.487(7) Å; **4**: 1.474(2) Å; **5**: 1.464(13) Å). Interestingly, the bowl depth in **5** (0.857(11) Å) is deeper than that in the parent molecule **1** and the "naked" dianion in **4** (Table 2). This may stem from the direct binding of Rb^+ ion to the convex face of $C_{28}H_{14}^{2-}$, as such metal coordination was previously seen to increase the bowl depth.[25] The calculated POAV angles (Table S4) are also consistent with the above-mentioned trend observed for the $C_{28}H_{14}^{2-}$ anion in **4** and **5**.

Table 2. Selected bond lengths in **1**, **4**, and **5** (in Å).

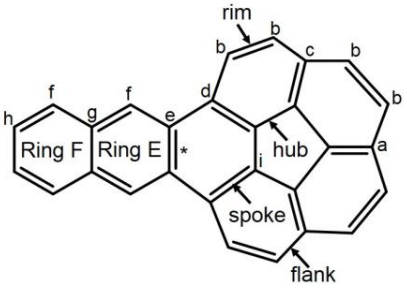

	1*	**4**	**5**
Rim	1.367(7)–1.390(7)Å	1.400(2)–1.425(2)Å	1.372(13)–1.404(9)Å
Hub	1.396(7)–1.442(7)Å	1.388(2)–1.422(2)Å	1.404(9)–1.423(9)Å
Flank	1.424(8)–1.474(7)Å	1.410(2)–1.474(2)Å	1.419(9)–1.471(9)Å
Spoke	1.350(8)–1.385(7)Å	1.390(2)–1.407(2)Å	1.388(10)–1.403(10)Å
Ring E	1.364(7)–1.487(7)Å	1.396(2)–1.474(2)Å	1.398(13)–1.464(13)Å
Ring F	1.356(8)–1.432(7)Å	1.384(2)–1.434(2)Å	1.375(11)–1.439(14)Å
Bowl Depth	0.813(7)	0.794(2)	0.857(11)

*Values are averaged for two naphthocorannulene cores in the independent unit.

Conclusions

We have accomplished the first comprehensive investigation of molecular and electronic structures, solid state packing and reduction properties of naphtho[2,3-*a*] corannulene ($C_{28}H_{14}$, **1**) and provided its direct comparison with parent corannulene ($C_{20}H_{10}$, **2**), using a combination of theoretical and experimental tools. The accessibility of two reduction steps for **1** was predicted theoretically and confirmed by cyclic voltammetry (CV) measurements, detecting two reversible one-electron reduction processes with the formal reduction potentials at –2.30 and –2.77 V *vs*. $Fc^{+/0}$. Both calculations and electrochemistry indicated that the HOMO-LUMO gap of **1** is reduced *vs*. that of **2**, making $C_{28}H_{14}$ a better acceptor than $C_{20}H_{10}$. The CV data also demonstrated the accessibility and stability of the corresponding mono- and dianionic states of **1**; and both were prepared using chemical reduction with Group 1 metals. The resulting products of the mono- and doubly-reduced naphtho[2,3-*a*] corannulene were crystallized as sodium and rubidium salts. Their X-ray diffraction study revealed the formation of "naked" mono- and dianions crystallized as solvent-separated ionic products with one or two sodium cations as $[Na^+(18\text{-crown-6})(THF)_2][C_{28}H_{14}^-]$ and [Na^+(18-crown-

6)(THF)$_2$]$_2$[$C_{28}H_{14}^{2-}$] (**3**·THF and **4**·THF, respectively). In addition, the dianion was isolated as a contact-ion complex with two rubidium countercations, [{Rb^+(18-crown-6)}$_2$($C_{28}H_{14}^{2-}$)] (**5**·THF). This structural characterization of **3**, **4** and **5** allowed the first evaluation of the outcomes of addition of one and two electrons to the carbon framework of naphtho[2,3-*a*] corannulene.

Experimental Section

Materials and Methods. All manipulations were carried out using break-and-seal[26] and glove-box techniques under an atmosphere of argon. Tetrahydrofuran (THF) and hexanes were purchased from Pharmco-Aaper, dried over Na/benzophenone and distilled prior to use. THF-d_8 was purchased from Sigma Aldrich, dried over NaK_2 alloy and vacuum-transferred. Sodium and rubidium metals were purchased from Strem Chemicals and used as received. Crown ether, 18-crown-6 (99%), was purchased from Sigma Aldrich and dried over P_2O_5 *in vacuo* for 24 hours. Naphtho[2,3-*a*]corannulene ($C_{28}H_{14}$, **1**) was prepared as described previously[14] and sublimed *in vacuo* in a sealed glass ampoule (5 inch length) at 160-180 °C prior to use. The UV-vis spectra were recorded on a PerkinElmer Lambda 35 spectrometer. The NMR spectra were measured on a Bruker AC-400 spectrometer at 400 MHz for ^{1}H and referenced to the resonances of the corresponding solvent used. For CV measurements (see ESI for more details), electrochemical or analytical grade tetrabutylammonium hexafluorophosphate (TBAH) from Sigma-Aldrich was used as received as a supporting electrolyte. Tetrahydrofuran (LiChrosolv, Merck) was purified and dried by sodium anthracenide in order to remove any traces of water, proton donors and oxygen as previously reported,[27] stored in a specially designed Schlenk flask and protected from light. The solvent was distilled via a closed system into a custom designed electrochemical cell containing the supporting electrolyte and the species under examination, immediately before performing the experiment.

Calculations: Geometry optimizations for all systems under consideration were performed at the DFT level of theory using hybrid functional PBE0[28] in combination with the correlation-consistent basis set cc-pVTZ applied to all atoms. No symmetry restrictions were used. All calculated structures are local minima on the corresponding potential energy surfaces. All calculations were done with help of the Firefly[29] program package (version 8.1.0). Electronic

structure was analyzed with help of NBO technique.[30] Using PBE0/cc-pVTZ-optimized geometries, a set of theoretical descriptors/indexes of aromaticity was calculated. This set includes: (*i*) structure-based Harmonic Oscillator Model of Aromaticity (HOMA, as defined by Kruszewsk and Krygowski,[31] (*ii*) Nuclear Independent Chemical Shift (NICS, introduced by von Rague Schleyer *et al*.[32] and (*iii*) descriptors based on topological Quantum Theory of Atom in Molecule (QTAIM) approach[33] such as Para-Delocalized Index (PDI)[34] and Aromatic Fluctuation Index (FLU).[35] All QTAIM calculations were carried out by Multiwfn 3.3.7 program.[36] Calculations of NICS values were performed using the Gauge Independent Atomic Orbitals (GIAO) approach with help of Gaussian 09 program[37] at the PBE0/cc-pVTZ level of theory. The set of descriptors was augmented by detailed consideration of magnetic induced ring current in target systems using Anisotropy of the Induced Current Density (ACID) approach.[38] To obtain induced the current vectors and plot map, ACID 2.0.0 program uses the current density tensors, calculated by the Continuous Set of Gauge Transformations (CSGT) method implemented in Gaussian 09 package.[39]

Crystallization of $C_{28}H_{14}$ (1): Deposition of **1** (5 mg, 0.014 mmol) at 160 °C in a sealed evacuated glass ampule over 2 days afforded yellow needle-shaped crystals in high yield (4.3 mg, 86 %).

Preparation of $[Na(18\text{-crown-6})(THF)_2]^+[C_{28}H_{14}^-]$ (3·THF): THF (1.0 mL) was added to a flask containing excess Na (0.2 mg, 0.008 mmol, 1.5 eq.), 18-crown-6 (1.5 mg, 0.0057 mmol) and naphthocorannulene (2 mg, 0.0057 mmol). The initial color of the mixture was pale yellow (neutral ligand), but within a few minutes the color turned brown. The reaction mixture was stirred for an additional 25 min and filtered; the brown filtrate was layered with hexanes (1.5 mL) and placed at 5 °C. Dark brown blocks were present in good yield after 4 days. Yield: 2.8 mg, 65%. UV/vis (THF): λ_{max} 373, 395, 405, 427, 493, 520, 555, 655 and 718 nm.

Preparation of $[Na^+(18\text{-crown-6})(THF)_2]_2[C_{28}H_{14}^{2-}]$ (4·THF): THF (1.5 mL) was added to a flask containing excess Na (1.1 mg, 0.046 mmol, 8 eq.), 18-crown-6 (3 mg, 0.0114 mmol) and naphthocorannulene (2 mg, 0.0057 mmol). The initial color of the mixture was pale yellow (neutral ligand). Within a few minutes, the color turned to dark brown and then to green (in *ca*. 30 min). After a total of 24 h of stirring, the resulting green suspension was filtered; the green filtrate was layered with hexanes (1.7 mL) and placed at 5 °C. Dark blocks were present in high yield after 4 days. Yield: 4.7 mg, 70%. UV/vis (THF): λ_{max} 586 and 692 nm.

Preparation of [{Rb^+(18-crown-6)}$_2$($C_{28}H_{14}^{2-}$)] (5·THF): THF (1.5 mL) was added to a flask containing excess Rb (3.1 mg, 0.036 mmol, 5 eq.), 18-crown-6 (3.8 mg, 0.014 mmol), and naphthocorannulene (2.5 mg, 0.007 mmol). The initial color of the mixture was pale yellow. Within a few minutes, the color of the mixture turned dark brown. The reaction mixture was stirred for an additional 10 minutes at room temperature, resulting in a dull brown-green suspension. After 20 minutes of stirring, the mixture was filtered; the brown-green filtrate was layered with hexanes (1.2 mL) and placed at 5 °C. Dark blocks were present in good yield after 4 days. Yield: 5.4 mg, 68%. UV/vis (THF): λ_{max} 475 and 692 nm. ^{1}H NMR (THF-d_8, 20 °C): δ = 3.67 (16H, 18-crown-6), 5.62 (1H, $C_{28}H_{14}^{2-}$), 6.61-6.69 (2H, $C_{28}H_{14}^{2-}$), 6.81 (1H, $C_{28}H_{14}^{2-}$), 7.11-7.18 (2H, $C_{28}H_{14}^{2-}$), 7.37-7.60 (7H, $C_{28}H_{14}^{2-}$), 8.05 (1H, $C_{28}H_{14}^{2-}$).

Note: The extreme air- and moisture sensitivity of crystals **3**–**5**, along with the presence of interstitial THF molecules, prevented obtaining of elemental analysis data.

Crystal structure determination and refinement: The single crystal diffraction data set of **1** was measured on a Bruker SMART APEX CCD-based X-ray diffractometer system equipped with a Mo-target X-ray tube (λ = 0.71073 Å) at T = 100(2) K and data collections of **3** and **4** were performed on a Bruker D8 VENTURE X-ray diffractometer with PHOTON 100 CMOS detector equipped with a Mo-target X-ray tube (λ = 0.71073 Å) at T = 100(2) K. Data collection of **5** was performed on a Bruker D8 VENTURE X-ray diffractometer with PHOTON 100 CMOS detector equipped with a Cu-target X-ray tube (λ = 1.54178 Å) at T = 100(2) K. Data reduction and integration were performed with the Bruker software package SAINT (version 8.37A).[40] Data were corrected for absorption effects using the empirical methods as implemented in SADABS (version 2016/2).[41] The structures were solved by SHELXT and refined by full-matrix least-squares procedures using the SHELXL (version 2016/6)[42] software package. CCDC 1584450 (**1**), 1584451 (**3**), 1584452 (**4**), and 1584453 (**5**) contain the supplementary crystallographic data for this paper. These data are provided free of charge by the Cambridge Crystallographic Data Centre. Further crystal data collection and structure refinement details are listed in supporting information and in Table S1.

Acknowledgements

M. A. P. gratefully acknowledges financial support of this work from the National Science Foundation (CHE-1608628 and MRI-1337594). A. Yu. R. acknowledges the support from the

Illinois Institute of Technology (IIT) through startup funding and partial support from the 381688-FSU/ChemRing/DOD-DOTC. M. M. acknowledges support from the University of Bologna. We also thank Mr. M. Ihde for crystallization of **1**, Dr. A. S. Filatov for collection of the X-ray diffraction data for **1**, and Dr. A. A. Granovsky with the Firefly team for providing the developing version of the Firefly program package.

References

[1] a) C. A. Reed, R. D. Bolskar, *Chem. Rev.* **2000**, *100*, 1075-1120; b) Y. Iwasa, *Nature* **2010**, *466*, 191-192; c) A. Y. Ganin, Y. Takabayashi, P. Jeglic, D. Arcon, A. Potocnik, P. J. Baker, Y. Ohishi, M. T. McDonald, M. D. Tzirakis, A. McLennan, G. R. Darling, M. Takata, M. J. Rosseinsky, K. Prassides, *Nature* **2010**, *466*, 221-225; d) K. Y. Amsharov, Y. Kramer, M. Jansen, *Angew. Chem. Int. Ed.* **2011**, *50*, 11640-11643; e) A. Kromer, U. Wedig, E. Roduner, M. Jansen, K. Y. Amsharov, *Angew. Chem. Int. Ed.* **2013**, *52*, 12610-12614; f) A. Potocnik, A. Y. Ganin, Y. Takabayashi, M. T. McDonald, I. Heinmaa, P. Jeglic, R. Stern, M. J. Rosseinsky, K. Prassides, D. Arcon, *Chem. Sci.* **2014**, *5*, 3008-3017; g) A. M. Rice, W. B. Fellows, E. A. Dolgopolova, A. B. Greytak, A. K. Vannucci, M. D. Smith, S. G. Karakalos, J. A. Krause, S. M. Avdoshenko, A. A. Popov, N. B. Shustova, *Angew. Chem. Int. Ed*. **2017**, *56*, 4525-4529.

[2] a) O. Vostrowsky, A. Hirsch, *Angew. Chem. Int. Ed.* **2004**, *43*, 2326-2329; b) M. N. Chaur, F. Melin, A. L. Ortiz, L. Echegoyen, *Angew. Chem. Int. Ed*. **2009**, *48*, 7514-7538; c) Y.-Z. Tan, S.-Y. Xie, R.-B. Huang, L.-S. Zheng, *Nat. Chem.* **2009**, *1*, 450-460; d) F. L. Bowles, M. M. Olmstead, A. L. Balch, *J. Am. Chem. Soc*. **2014**, *136*, 3338-3341; e) D. V. Konarev, S. S. Khasanov, R. N. Lyubovskaya, *Coord. Chem. Rev.* **2014**, *262*, 16-36; f) A. L. Balch, K. Winkler, *Chem. Rev.* **2016**, *116*, 3812-3882.

[3] a) L. T. Scott, H. E. Bronstein, D. V. Preda, R. B. M. Ansems, M. S. Bratcher, S. Hagen, *Pure Appl. Chem.* **1999**, *71*, 209-219; b) L. T. Scott, *Angew. Chem. Int. Ed.* **2004**, *43*, 4994-5007; c) V. M. Tsefrikas, L. T. Scott, *Chem. Rev.* **2006**, *106*, 4868-4884; d) T. J. Hill, R. K. Hughes, L. T. Scott, *Tetrahedron* **2008**, *64*, 11360-11369; e) L. T. Scott, *Polycyclic Aromat. Compd.* **2010**, *30*, 247-259; f) N. Martin, L. T. Scott, *Chem. Soc. Rev.* **2015**, *44*, 6397-6400.

[4] A. Sygula, *Eur. J. Org. Chem.* **2011**, 1611-1625.

[5] Y.-T. Wu; J. S. Siegel, *Chem. Rev*. **2006**, *106*, 4843-4867.

[6] T. Amaya, T. Hirao, *Chem. Rec*. **2015**, *15*, 310-321.

[7] a) A. S. Filatov, M. A. Petrukhina, *Coord. Chem. Rev*. **2010**, *254*, 2234-2246; b) *Fragments of Fullerenes and Carbon Nanotubes: Designed Synthesis, Unusual Reactions, and Coordination Chemistry* (Eds: M. A. Petrukhina, L. T. Scott), Wiley, Hoboken, New Jersey, **2012**, pp. 413; c) A. V. Zabula, M. A. Petrukhina, *Adv. Organomet. Chem*. **2013**, *61*, 375-462.

[8] a) A. Ayalon, M. Rabinovitz, P.-C. Cheng, L. T. Scott, *Angew. Chem. Int. Ed.* **1992**, *31*, 1636-1637; b) A. Ayalon, A. Sygula, P.-C. Cheng, M. Rabinovitz, P. W. Rabideau, L. T. Scott, *Science* **1994**, *265*, 1065-1067; c) M. Baumgarten, L. Gherghel, M. Wagner, A. Weitz, M. Rabinovitz, P.-C. Cheng, L. T. Scott, *J. Am. Chem. Soc.* **1995**, *117*, 6254-6257.

[9] a) S. N. Spisak, A. V. Zabula, A. S. Filatov, A. Yu. Rogachev, M. A. Petrukhina, *Angew. Chem. Int. Ed.* **2011**, *50*, 8090-8094; b) A. V. Zabula, S. N. Spisak, A. S. Filatov, V. M. Grigoryants, M. A. Petrukhina, *Chem. Eur. J.* **2012**, *18*, 6476-6484; c) S. N. Spisak, A. V. Zabula, M. V. Ferguson, A. S. Filatov, M. A. Petrukhina, *Organometallics* **2013**, *32*, 538-543; d) S. N. Spisak, N. J. Sumner, A. V. Zabula, A. S. Filatov, A. Yu. Rogachev, M. A. Petrukhina, *Organometallics* **2013**, *32*, 3773-3779; e) S. N. Spisak, A. V. Zabula, A. S. Filatov, M. A. Petrukhina, *J. Organomet. Chem.* **2015**, *784*, 69-74.

[10] a) A. V. Zabula, A. S. Filatov, S. N. Spisak, A. Yu. Rogachev, M. A. Petrukhina, *Science* **2011**, *333*, 1008-1011; b) A. V. Zabula, S. N. Spisak, A. S. Filatov, M. A. Petrukhina, *Organometallics* **2012**, *31*, 5541-5545; c) A. V. Zabula, S. N. Spisak, A. S. Filatov, M. A. Petrukhina, *Angew. Chem. Int. Ed.* **2012**, *51*, 12194-12198; d) A. S. Filatov, A. V. Zabula, S. N. Spisak, A. Yu. Rogachev, M. A. Petrukhina, *Angew. Chem. Int. Ed.* **2014**, *53*, 140-145; e) A. S. Filatov, S. N. Spisak, A. V. Zabula, J. McNeely, A. Yu. Rogachev, M. A. Petrukhina, *Chem. Sci.* **2015**, *6*, 1959-1966; f) A. V. Zabula, S. N. Spisak, A. S. Filatov, A. Yu. Rogachev, R. Clérac, M. A. Petrukhina, *Chem. Sci.* **2016**, *7*, 1954-1961; e) S. N. Spisak, A. Yu. Rogachev, A. V. Zabula, A. S. Filatov, R. Clérac, M. A. Petrukhina. *Chem. Sci*. **2017**, *8*, 3137-3145.

[11] S. N. Spisak, Z. Wei, N. J. O'Neil, A. Yu. Rogachev, T. Amaya, T. Hirao, M. A. Petrukhina, *J. Am. Chem. Soc.* **2015**, *137*, 9768-9771.

[12] a) S. N. Spisak, J. Li, A. Yu. Rogachev, Z. Wei, O. Papaianina, K. Amsharov, A. V. Rybalchenko, A. A. Goryunkov, M. A. Petrukhina, *Organometallics* **2016**, *35*, 3105-3111; b) Q. Xu, M. A. Petrukhina, A. Yu. Rogachev, *PCCP* **2017**, *19*, 21575-21583.

[13] a) W. Clegg, S. H. Dale, E. Hevia, L. M. Hogg, G. W. Honman, R. E. Mulvey, C. T. O'Hara, *Angew. Chem. Int. Ed.* **2006**, *45*, 6548-6550; b) T. A. Scott, B. A. Ooro, D. J. Collins, M. Shatruk, A. Yakovenko, K. R. Dunbar, H.-C. Zhou, *Chem. Commun.* **2009**, 65-67; c) C. Melero, A. Guijarro, M. Yus, *Dalton. Trans*. **2009**, 1286-1289.

[14] D. V. Preda, *New Chemistry and Annulations of Corannulene*, Ph.D. Thesis, Boston College, **2001**.

[15] I. Aprahamian, D. V. Preda, M. Bancu, A. P. Belanger, T. Sheradsky, L. T. Scott, M. Rabinovitz, *J. Org. Chem.* **2006**, *71*, 290-298.

[16] a) A. K. Dutta, A. Linden, L. Zoppi, K. K. Baldridge, J. S. Siegel, *Angew. Chem. Int. Ed.* **2015**, *54*, 10792-10796; b) V. Rajeshkumar, M. Courté, D. Fichou, M. C. Stuparu, *Eur. J. Org. Chem.* **2016**, 6010-6014.

[17] M. A. Petrukhina, K. W. Andreini, J. Mack, L. T. Scott, *J. Org. Chem.* **2005**, *70*, 5713-5716.

[18] a) E. Clar, *Polycyclic Hydrocarbons*, Academic: London, **1964**. b) R. G. Harvey, *Polycyclic Aromatic Hydrocarbons*, Wiley-VCH: New York, **1997**.

[19] C. Bruno, R. Benassi, A. Passalacqua, F. Paolucci, C. Fontanesi, M. Marcaccio, E. A. Jackson, L. T. Scott, *J. Phys. Chem. B* **2009**, *113*, 1954-1962.

[20] a) M. A. Petrukhina, *Coord. Chem. Rev*. **2007**, *251*, 1690-1698. b) A. S. Filatov, M. A. Petrukhina, *Coord. Chem. Rev*. **2010**, *254*, 2234-2246; c) O. Hietsoi, A. S. Filatov, C. Dubceac, M. A. Petrukhina, *Coord. Chem. Rev***. 2015**, *295*, 125-138.

[21] a) D. Eisenberg, A. S. Filatov, E. Jackson, M. Rabinovitz, M. A. Petrukhina, L. T. Scott, R. Shenhar, *J. Org. Chem*. **2008**, *73*, 6073-6078; b) A. V. Zabula, Y. V. Sevryugina, S. N. Spisak, L. Kobryn, R. Sygula, A. Sygula, M. A. Petrukhina, *Chem. Commun*. **2014**, *50*, 2557-2659; c) C. Dubceac, A. S. Filatov, A. V. Zabula, M. A. Petrukhina, *Cryst. Growth Des*. **2015**, *15*, 778-785.

[22] a) M. A. Petrukhina, K. W. Andreini, V. M. Tsefrikas, L. T. Scott, *Organometallics* **2005**, *24*, 1394-1397; b) A. S. Filatov, L. T. Scott, M. A. Petrukhina, *Cryst. Growth Des*. **2010**, *10*, 4607-4621.

[23] S. N. Spisak, Z. Wei, A. Yu. Rogachev, T. Amaya, T. Hirao, M. A. Petrukhina, *Angew. Chem. Int. Ed*. **2017**, *56*, 2582-2587.

[24] a) S. Neander, U. Behrens, F. Olbrich, *J. Organomet. Chem.* **2000**, *604*, 59-67; b) T. Wombacher, R. Goddard, C. W. Lehmann, J. J. Schneider, *Chem. Comm*. **2017**, *53*, 7030-7033.

[25] A. S. Filatov, A. Yu. Rogachev, E. A. Jackson, L. T. Scott, M. A. Petrukhina, *Organometallics* **2010**, *29*, 1231-1237.

[26] N. V. Kozhemyakina, J. Nuss, M. Jansen, Z. *Anorg. Allg. Chem.* **2009**, *635*, 1355-1361.

[27] a) A. A. La Pensée, J. Bickley, S. J. Higgins, M. Marcaccio, F. Paolucci, S. Roffia, J. M. Charnock, *Dalton Trans.* **2002**, 4095-4104; b) F. Cecchet, A. M. Gioacchini, M. Marcaccio, F. Paolucci, S. Roffia, M. Alebbi, C. A. Bignozzi, *J. Phys. Chem. B* **2002**, *106*, 3926-3932.

[28] a) J. P. Perdew, K. Burke, M. Ernzerhof, *Phys. Rev. Lett.* **1997**, *78*, 1396; b) J. P. Perdew, K. Burke, M. Ernzerhof, *Phys. Rev. Lett.* **1996**, *77*, 3865-3868.

[29] A. A. Granovsky, Firefly version 8.1.0, http://classic.chem.msu.su/gran/firefly/index.html.

[30] a) A. E. Reed, L. A. Curtiss, F. Weinhold, *Chem. Rev.* **1988**, *88*, 899-926; b) *Valency and Bonding: A Natural Bond Orbital Donor−Acceptor Perspective* (Eds.: F. Weinhold, C. A. Landis) Cambridge University Press, Cambridge, **2005**; c) E. D. Glendening, J. K. Badenhoop, A. E. Reed, J. E. Carpenter, J. A. Bohmann, C. M. Morales, F. Weinhold, NBO 6.0, University of Wisconsin, Madison, **2013**; d) E. D. Glendening, C. R. Landis, F. Weinhold, *J. Comp. Chem.* **2013**, *34*, 1429-1437.

[31] a) J. Kruszewski, T. M. Krygowski, *Tetrahedron Lett*. **1972**, *13*, 3839-3842; b) T. M. Krygowski, *J. Chem. Inf. Comp. Sci.* **1993**, *33*, 70-78.

[32] a) P. von Ragué Schleyer, C. Maerker, A. Dransfeld, H. Jiao, N. J. R. van Eikema Hommes, *J. Am. Chem. Soc.* **1996**, *118*, 6317-6318; b) Z. Chen, C. S. Wannere, C. Corminboeuf, R. Puchta, P. von Ragua Schleyer, *Chem. Rev.* **2005**, *105*, 3842-3888.

[33] a) *Atoms in Molecules: A Quantum Theory* (Eds.: R. F. W. Bader), Clarendon Press, Oxford, **1990**; b) *The Quantum Theory of Atoms in Molecules* (Eds.: C. F. Matta, R. J. Boyd), Wiley-VCH, Verlag, **2007**.

[34] J. Poater, X. Fradera, M. Duran, M. Sola, *Chem. Eur. J*. **2003**, *9*, 400-406.

[35] E. Matito, M. Duran, M. Sola, *J. Chem. Phys*. **2005**, *122*, 014109/1-014109/8.

[36] T. Lu, F. Chen, *J. Comp. Chem*. **2012**, *33*, 580-592.

[37] M. J. Frisch, G. W. Trucks, H. B. Schlegel, G. E. Scuseria, M. A. Robb, J. R. Cheeseman, G. Scalmani, V. Barone, B. Mennucci, G. A. Petersson, H. Nakatsuji, M. Caricato, X. Li, H. P. Hratchian, A. F. Izmaylov, J. Bloino, G. Zheng, J. L. Sonnenberg, M. Hada, M. Ehara, K. Toyota, R. Fukuda, J. Hasegawa, M. Ishida, T. Nakajima, Y. Honda, O. Kitao, H. Nakai, T.

Vreven, J. A. Montgomery, Jr., J. E. Peralta, F. Ogliaro, M. Bearpark, J. J. Heyd, E. Brothers, K. N. Kudin, V. N. Staroverov, R. Kobayashi, J. Normand, K. Raghavachari, A. Rendell, J. C. Burant, S. S. Iyengar, J. Tomasi, M. Cossi, N. Rega, J. M. Millam, M. Klene, J. E. Knox, J. B. Cross, V. Bakken, C. Adamo, J. Jaramillo, R. Gomperts, R. E. Stratmann, O. Yazyev, A. J. Austin, R. Cammi, C. Pomelli, J. W. Ochterski, R. L. Martin, K. Morokuma, V. G. Zakrzewski, G. A. Voth, P. Salvador, J. J. Dannenberg, S. Dapprich, A. D. Daniels, Ö. Farkas, J. B. Foresman, J. V. Ortiz, J. Cioslowski, and D. J. Fox, Gaussian 09, Revision D.01, Gaussian, Inc., Wallingford CT, **2009.**

[38] R. Herges, D. Geuenich, *J. Phys. Chem. A* **2001**, *105*, 3214-3220.

[39] T. A. Keith, R. F. W. Bader, *Chem. Phys. Lett*. **1993**, *210*, 223-230.

[40] SAINT; part of Bruker APEX3 software package (version 2016.9-0): Bruker AXS, 2016.

[41] SADABS; part of Bruker APEX3 software package (version 2016.9-0): Bruker AXS, 2016.

[42] SHELXL refinement program version 2016/6: G. M. Sheldrick, *Acta Cryst.* **2015**, *C71*, 3-8.